Twisted fiber pullout from UHPC: A computational study

Yuh-Shiou Tai*, Ph.D., (corresponding author) – Research Scientist, Department of Civil & Environmental Engineering, University of Michigan, 2374 G.G. Brown, Ann Arbor, MI 48109-2125, USA, Phone: 734-629-6399, Email: taiyuh@umich.edu

Sherif El-Tawil, Ph.D., P.E., – Professor, Department of Civil & Environmental Engineering, University of Michigan, 2374 G.G. Brown, Ann Arbor, MI 48109-2125, USA, Phone: 734-764-5617, Email: eltawil@umich.edu

Abstract: A highly detailed computational model is developed to simulate the behavior of twisted steel fiber pullout from ultra-high-performance concrete (UHPC). The model considers the effect of fiber-matrix interfacial behavior and material inelasticity. It is shown that the model is capable of reproducing key experimental observations including the ability of twisted fibers to exhibit pseudo-plastic behavior for slip values up to 80%-90% of a fiber's embedded length. It is also shown that the maximum pullout decreases with increasing pitch and that fibers with triangular cross-section have a somewhat larger ability to dissipate energy than fibers with other cross-sectional shapes.

Keywords: fiber pullout; ultra-high strength concrete (UHPC); twisted steel fiber

1. Introduction

It is well known that the bond-slip relationship between fibers and the surrounding UHPC matrix directly influences the mechanical properties of the composite (Lee et al. 2010; Wille and Naaman 2012, 2013; Feng et al. 2014; Tai et al. 2016; Xu et al. 2016; Tai and El-Tawil 2017). The resistance that fibers offer against crack opening enables strain hardening tensile behavior and promotes multiple cracking (Pyo et al. 2015, 2016; Wille et al. 2012; Tran et al. 2016; Yoo and Banthia 2016; Benson and Karihaloo 2005; Alkaysi et al. 2016).

Fiber-matrix debonding and frictional sliding are the two primary resistance mechanisms governing the pullout behavior of straight fibers (Wille and Naaman 2012, 2013; Feng et al. 2014; Tai et al. 2016; Naaman et al. 1991; Armelin and Banthia 1997). Deformed steel fibers, on the other hand, mobilize mechanical anchorage during pullout, e.g. hooked and twisted fibers straighten and untwist, respectively, when pulled out (Wille and Naaman 2012, Feng et al. 2014; Tai et al. 2016; Xu et al. 2016; Tai and El-Tawil 2017).

The mechanical anchorage part of deformed steel fibers has been the subject of numerous studies in the past (Alwan et al. 1999; Sujivorakul et al. 2000; Kim et al. 2010; Cunha et al. 2009; Guerrero and Naaman 2000; Wille et al. 2011; Sujivorakul 2002). Twisted fibers, in particular, have been studied extensively in the context of high performance cementitious composites (Sujivorakul 2002; Naaman 1998; Sujivorakul and Naaman 2002), although pullout studies from UHPC are rare.

Experimental pullout studies by Naaman et al. (Naaman 1998; Sujivorakul and Naaman 2002) suggest that the factors that affect bond-slip performance of twisted fibers are cross-

sectional shape, twist pitch, mechanical properties of the matrix and fiber, and embedment length. Tai et al. (2016) investigated the effect of loading rates and in a related study, Tai and El-Tawil (2017) investigated the rate-dependent pullout behavior of twisted fibers at different inclination angles. Other experimental studies can be found in Xu et al. (2016) and Park et al. (2014). Analytical studies of twisted fiber pullout behavior have also been published, e.g. in Naaman et al. (1998, 2002, 2010]. Simulation studies of twisted fiber pullout behavior are quite rare, e.g. Ellis et al. (2014).

The above survey shows that very little computational work has been conducted to study the pullout behavior of twisted fibers from UHPC matrices. Motivated by this and the widespread interest in UHPC, this study seeks deep insight into twisted fiber pullout behavior from UHPC. The research is conducted using computational simulation at the scale of a single fiber. The simulations address a range of parameters that go beyond those considered in other experimental and computational studies.

2. Finite Element Modeling of the Pullout Test

The finite element model of the pullout setup in Fig. 1 is shown in Fig. 2. The model was created in Hypermesh (2011) and the simulations were performed with LS-Dyna. Only the necessary portion of test setup is represented for computational expediency. A spring was introduced at the base of the specimen to account for the flexibility of the testing system. The UHPC matrix part and twisted steel fiber are finely discretized using tetrahedral elements and the automatic single surface contact algorithm is employed to prevent interpenetration.
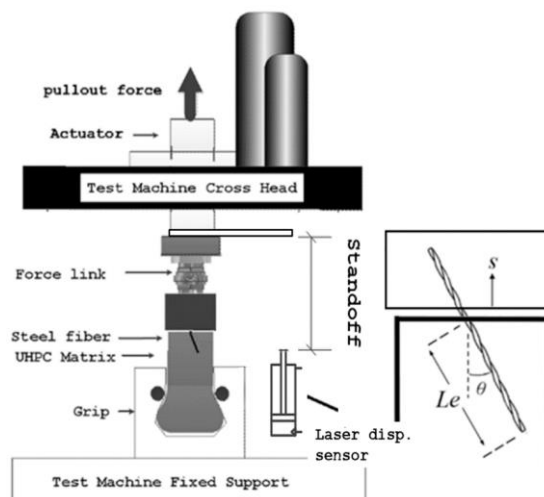

Fig. 1. Experimental pullout setup

2.1. UHPC Model

The behavior of UHPC elements was modeled using MAT072 (Magallanes et al. 2010). Kunnath et al. (2018) investigated the performance MAT072 and showed that it had the ability to reproduce critical features of concrete response. The compressive, tensile strength and Young's modulus of the UHPC matrix used in this study were 185 MPa, 7.4 MPa and 49.1 GPa, respectively. The three strength surface (initial yield, maximum, and residual surface) parameters were automatically generated by the program. However, it was necessary to calibrate the parameters b_1 and b_2 that control the softening damage evolution in compression and tension to reflect the actual brittle

nature of UHPC matrix. The values of b_1 and b_2 used in this study were 1.6 and 4.5, respectively. The shear dilatancy factor controls the volumetric expansion and was taken as 0.75 for concrete without confinement pressure according to Crawford et al. (2012).
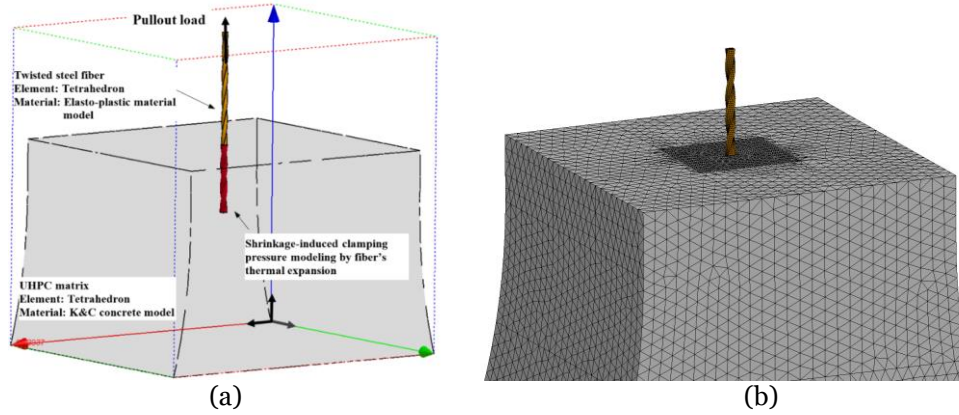

(a)   (b)
Fig. 2. Model of aligned fiber pullout setup

2.2. Steel Fiber Model

Tensile tests were conducted to obtain the tensile properties of the steel fibers. The average of three specimens showed that Young's modulus was 176.2 GPa and that the yielding stress and tensile strength were 1569 MPa and 2000 MPa, respectively. Elements are assumed to fracture when the ultimate strain reaches 0.018 in order to match the fracture behavior seen in the test.

2.3. Interfacial Bond Model

Interfacial bond is governed by adhesion and friction. The former is lost quickly upon initiation of pullout, leaving the latter as the dominant source of resistance. Adhesion is typically quite small compared to the frictional and mechanical components of bond resistance and is therefore ignored in this work. UHPC has a low water-to-binder ratio and incorporates silica fume, both of which contribute to high shrinkage and confinement of the fibers. A Coulomb friction model was employed to account for this confinement effect.

Instead of explicitly modeling the confinement effect introduced by shrinkage, it is more convenient to represent the process by assuming that the fiber's temperature increases. The increase in temperature causes the fiber to expand, pushing against the surrounding matrix and creating confinement stresses, activating the Coulomb model.

3. Model Calibration

The needed initial temperature rise is computed by calibrating the model's results to experimental data in (Tai et al. 2016) for smooth, straight fibers for a coefficient of friction of 0.5. Figure 3 shows the computed pullout curve compared against that obtained from experiments. The tests used 0.2 mm diameter brass-coated steel fibers and the embedded length was 6 mm. The computed pullout response is plotted for various heating temperatures (60 ℃, 90 ℃ and 120 ℃). Of the three

computed curves, the one associated with a 90 °C temperature increase was judged best in terms of initial response, peak load and post peak response and used in subsequent analyses.

The stiffness of the spring attached to the specimen's base (to account for the flexibility of the test system) was also calibrated to the test data in (Tai et al. 2016) for aligned, straight, smooth fibers. The calibration results indicated that the intial stiffness of the spring is 650 N/mm.
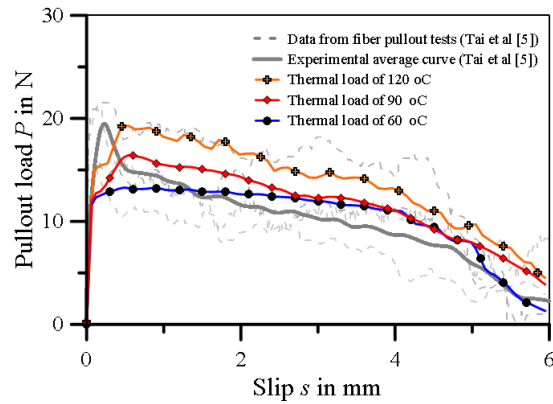

Fig. 3 Effect of temperature rise (to model friction effects) on the pullout load versus slip relationship for aligned, straight smooth fibers

4. Model Validation

Validation is conducted using data for twisted fibers in (Tai and El-Tawil 2017), tested in both aligned and inclined configurations. Fig. 4 illustrates the pullout load versus the relative end slip responses of aligned and inclined (15-degree inclination) twisted fibers, respectively, obtained from experiments (Tai and El-Tawil 2017) and numerical analyses. It can be seen from Fig. 4 that the initial ascent segments for the inclined and aligned fibers are almost linear up to the debonding point. This excellent bonding behavior is attributed to the frictional and mechanical bond components working together to resist initial fiber pullout. As the fiber untwisting behavior is mobilized, which is fully plastic, the simulation results match the experimental results in that the pullout load plateaus then drops at low rate up to large slip values.
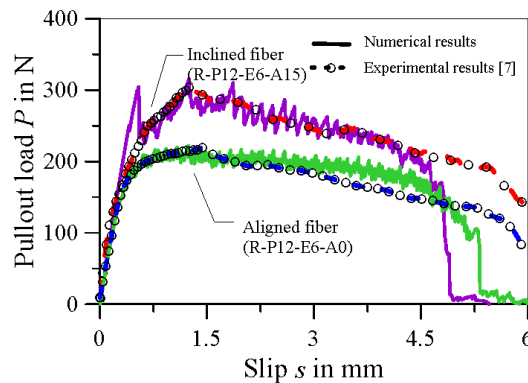

Fig. 4 Model validation. Comparison between pullout load v.s. slip responses of aligned and inclined fibers

5. Results and discussions

The effects of cross-section (rectangular, square, and triangular) and pitch (8 mm, 12 mm and 16 mm) on the response of a twisted fiber embedded in the UHPC matrix were investigated using the validated model. The naming scheme is C-P, where C is the cross-sectional shape (e.g. rectangular (R), square (S), and triangular (T)); P is the pitch (e.g. 8mm, 12mm, 16mm). For example, R-P8 means rectangular fiber with a pitch distance of 8mm. Nine simulations in total were performed (three cross-sections times three pitches). The sections were selected such that the rectangular, square and triangular sections fit inside the same circle and have the same area (0.245 mm^2). All three have approximately the same fiber intrinsic efficiency ratio (ranging between 48 and 55), which was defined by Naaman (2003) as the ratio of the bonded lateral surface area of the fiber to its cross-sectional area.

5.1 General Response

The results of all the pullout cases are shown in Figure 5. Figures 5(a) show the cases of R-P8, R-P12 and R-P16 pullout force development versus relative slip for three different pitches: 8 mm, 12 mm and 16 mm. It can be seen from Figures 5(a) that the pitch has a significant effect on pullout resistance. In particular, fibers with smaller pitch, e.g. R-P8 develop a higher pull-out force and bond shear stresses than the fibers with greater pitch. The improved strength is attributed to the presence of a greater number of twisted ribs per unit length compared to the other fibers, which causes a larger contact area between the fiber and surrounding matrix and, hence, greater frictional resistance.
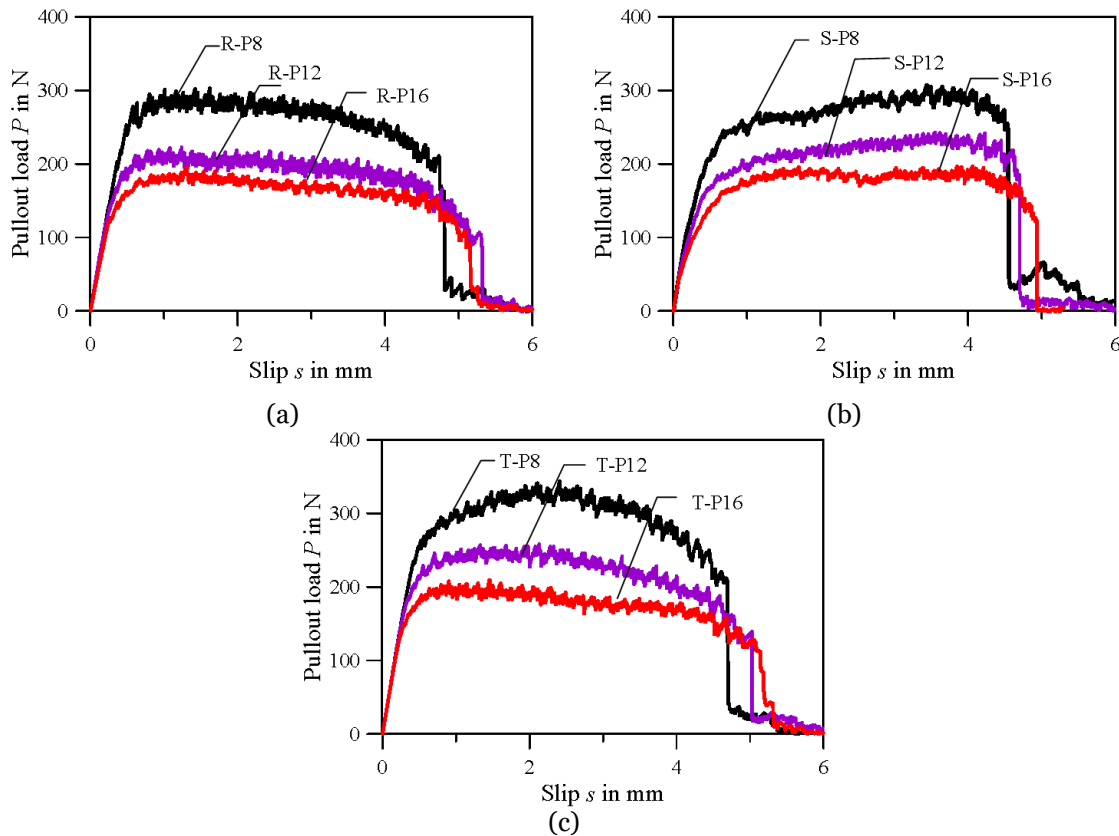

Fig. 5 Twisted steel fiber with rectangular cross-sectional pullout response (a) R-fibers; (b) S-fibers, (c) T-fibers

5.2 Influence of Fiber Cross-Section Shape

The pull-out load development as a function of slip are shown in Fig. 5(b) and Fig. 5(c) for fibers with square and triangular cross sections, respectively. The overall trend is comparable to the pullout response observed for fibers with rectangular cross-section. The results from these figures show that a high-level of pullout load is maintained up to a large slip distance, which is about 70% to 90% of the embedded length. Such results have also been observed in previous experimental studies (Tai et al. 2017, Sujivorakul 2002, Kim et al. 2010), although those studies used different fiber geometries and matrix strengths. This favorable mechanism is mainly attributed to the wedging effect between the matrix and the twisted part of the fiber embedded in it and the continuous untwisting that takes place along the fiber after initial debonding.

Fig. 6 illustrates the pullout force responses at different phases, including initial debonding, at a slip distance of 1 mm, and peak pullout force. As shown in Fig. 6, cases R-P8, S-P8 and T-P8 have initial debonding loads of 202.9 N, 184.0 N, and 232.0, respectively. At 1.0 mm slip, the corresponding pullout loads are 293.8 N, 246.0 N and 296.0 N, respectively. The corresponding peak loads are 303.0 N, 308.0 N, and 344.0 N. The computational results show that the contribution of untwisting for the T- fiber during the pullout process is more significant than that for the R- and S- fibers.
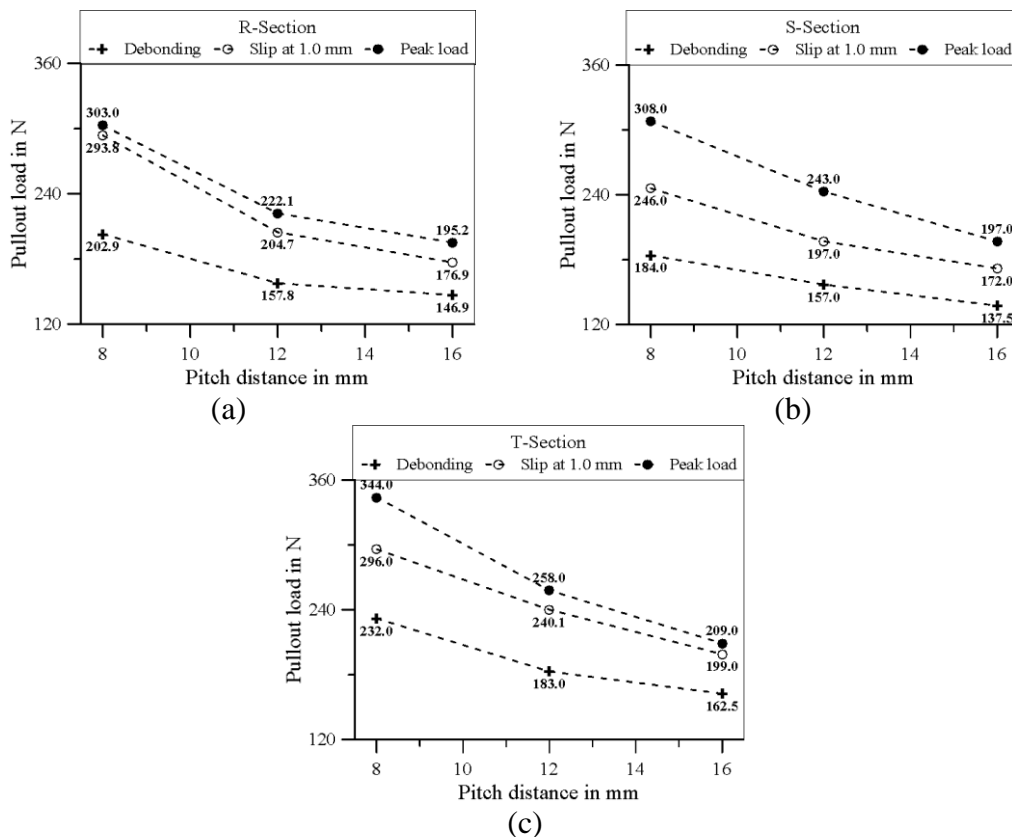

(a)

(b)

(c)

Fig. 6 Pullout force at different loading stages (a) R-fiber; (b) S-fiber; (c) T-fiber

6. Conclusions

A computational study was conducted to investigate the pullout behavior of twisted steel fibers from a UHPC matrix. Interfacial friction was simulated by raising the temperature of the fiber so that it expanded against the surrounding matrix, creating bearing stresses. The contact model employed prevented interpenetration of steel and matrix nodes elements and represented the interfacial response through a Coulomb friction model. The model was calibrated and validated using experimental data. The results of the simulations show that the maximum pullout decreased with increasing pitch and that T-fibers have the largest energy dissipation capacity followed by R-fibers and then S-fibers.

7. References

Alkaysi, Mo, et al. "Effects of silica powder and cement type on durability of ultra high performance concrete (UHPC)." Cement and Concrete Composites 66 (2016): 47-56.

Alwan, Jamil M., Antoine E. Naaman, and Patricia Guerrero. "Effect of mechanical clamping on the pull-out response of hooked steel fibers embedded in cementitious matrices." Concrete Science and Engineering 1.1 (1999): 15-25.

Armelin, Hugo S., and Nemkumar Banthia. "Predicting the flexural postcracking performance of steel fiber reinforced concrete from the pullout of single fibers." Materials Journal 94.1 (1997): 18-31.

Benson, S. D. P., and B. L. Karihaloo. "CARDIFRC®-Development and mechanical properties. Part III: Uniaxial tensile response and other mechanical properties." Magazine of Concrete Research 57.8 (2005): 433-443.

Brannon, R.M. and S. Leelavanichkul, Survey of four damage models for concrete, Sandia National Laboratories, 32(2009) 1-80.

Computing, Altair. "Hypermesh Version 11.0." Altair Engineering Inc. Troy, MI (2011).

Crawford, J. E., et al. "Use and validation of the release III K&C concrete material model in LS-DYNA." Karagozian & Case, Glendale (2012).

Cunha, Vítor MCF, Joaquim AO Barros, and José M. Sena-Cruz. "Pullout behavior of steel fibers in self-compacting concrete." Journal of Materials in Civil Engineering 22.1 (2009): 1-9.

Ellis, B. D., D. L. McDowell, and M. Zhou. "Simulation of single fiber pullout response with account of fiber morphology." Cement and Concrete Composites 48 (2014): 42-52.

Feng, J., et al. "Mechanical analyses of hooked fiber pullout performance in ultra-high-performance concrete." Construction and Building Materials 69 (2014): 403-410.

Guerrero, Patricia, and Antoine E. Naaman. "Effect of mortar fineness and adhesive agents on pullout response of steel fibers." Materials Journal 97.1 (2000): 12-20.

Kim, D. Joo, S. El-Tawil, and A. E. Naaman. "Effect of matrix strength on pullout behavior of high-strength deformed steel fibers." ACI: Special Publication 272 (2010): 135-150.

Kunnath, Sashi K., Yihai Bao, and Sherif El-Tawil, "Advances in computational simulation of gravity-induced progressive collapse of RC Frame Buildings," J. Struct. Eng. ASCE, 144 (2018): 1-18.

Lee, Yun, Su-Tae Kang, and Jin-Keun Kim. "Pullout behavior of inclined steel fiber in an ultra-high strength cementitious matrix." Construction and Building Materials 24.10 (2010): 2030-2041.

Magallanes, Joseph M., et al. "Recent improvements to release III of the K&C concrete model." 11th international LS-DYNA Users conference. Livermore Software Technology Corporation Livermore, CA, 2010.

Naaman, Antoine E., et al. "Fiber pullout and bond slip. I: Analytical study." Journal of Structural Engineering 117.9 (1991): 2769-2790.

Naaman, Antoine E. "New Fiber Technology (Cement, Ceramic, and Polymeric Composites)." Concrete International 20.7 (1998): 57-62.

Naaman, Antoine E. "Engineered steel fibers with optimal properties for reinforcement of cement composites." Journal of advanced concrete technology 1.3 (2003): 241-252.

Park, Seung Hun, et al. "Effect of shrinkage reducing agent on pullout resistance of high-strength steel fibers embedded in ultra-high-performance concrete." Cement and Concrete Composites 49 (2014): 59-69.

Pyo, Sukhoon, et al. "Strain rate dependent properties of ultra high performance fiber reinforced concrete (UHP-FRC) under tension." Cement and Concrete Composites 56 (2015): 15-24.

Pyo, Sukhoon, Sherif El-Tawil, and Antoine E. Naaman. "Direct tensile behavior of ultra high performance fiber reinforced concrete (UHP-FRC) at high strain rates." Cement and Concrete Research 88 (2016): 144-156..

Sujivorakul, C., A. M. Waas, and A. E. Naaman. "Pullout response of a smooth fiber with an end anchorage." Journal of Engineering Mechanics126.9 (2000): 986-993.

Sujivorakul, C., and A. E. Naaman. "Evaluation of bond-slip behavior of twisted wire strand steel fibers embedded in cement matrix." Special Publication 206 (2002): 271-292.

Sujivorakul, C. Development of high performance fiber-reinforced cement composites using twisted polygonal steel fibers. Diss. 2002.

Tai, Yuh-Shiou, and Sherif El-Tawil. "High loading-rate pullout behavior of inclined deformed steel fibers embedded in ultra-high performance concrete." Construction and Building Materials 148 (2017): 204-218.

Tai, Yuh-Shiou, Sherif El-Tawil, and Ta-Hsiang Chung. "Performance of deformed steel fibers embedded in ultra-high performance concrete subjected to various pullout rates." Cement and Concrete Research 89 (2016): 1-13.

Tran, Ngoc Thanh, et al. "Fracture energy of ultra-high-performance fiber-reinforced concrete at high strain rates." Cement and Concrete Research 79 (2016): 169-184.

Wille, Kay, and Antoine E. Naaman. "Effect of ultra-high-performance concrete on pullout behavior of high-strength brass-coated straight steel fibers." ACI Materials Journal 110.4 (2013): 451-461.

Wille, Kay, and Antoine E. Naaman. "Pullout Behavior of High-Strength Steel Fibers Embedded in Ultra-High-Performance Concrete." ACI Materials Journal 109.4 (2012): 479-488.

Wille, Kay, Antoine E. Naaman, and Gustavo J. Parra-Montesinos. "Ultra-High Performance Concrete with Compressive Strength Exceeding 150 MPa (22 ksi): A Simpler Way." ACI Materials Journal 108.1 (2011): 46–54.

Wille, Kay, et al. "Ultra-high performance concrete and fiber reinforced concrete: achieving strength and ductility without heat curing." Materials and structures 45.3 (2012): 309-324.

Xu, Man, Bryan Hallinan, and Kay Wille. "Effect of loading rates on pullout behavior of high strength steel fibers embedded in ultra-high performance concrete." Cement and Concrete Composites 70 (2016): 98-109.

Yoo, Doo-Yeol, and Nemkumar Banthia. "Mechanical properties of ultra-high-performance fiber-reinforced concrete: A review." Cement and Concrete Composites 73 (2016): 267-280.
.